Analytica Chimica Acta 889 (2015) 113–122

Contents lists available at ScienceDirect

Analytica Chimica Acta

journal homepage: www.elsevier.com/locate/aca

Catalytic amplification based on hole-transporting materials as efficient metal-free electrocatalysts for non-enzymatic glucose sensing

Yue Gu [a], Rongrong Yuan [b], Xiaoyi Yan [a], Cong Li [a], Weilu Liu [c], Ruixue Chen [a], Liu Tang [a], Bo Zheng [a], Yaru Li [a], Zhiquan Zhang [a,*], Ming Yang [d,**]

[a] College of Chemistry, Jilin University, Changchun 130012, PR China
[b] State Key Laboratory of Inorganic Synthesis and Preparative Chemistry, College of Chemistry, Jilin University, Changchun 130012, PR China
[c] School of Pharmacy, Shenyang Pharmaceutical University, Shenyang 110016, PR China
[d] Department of Breast Surgery, First Hospital, Jilin University, Changchun 130012, PR China

HIGHLIGHTS

- Hole-transporting material was used as a signal amplifier in designing glucose sensor.
- This metal-free electrocatalyst showed excellent catalytic activity toward glucose.
- Wide linear range and low detection potential for glucose determination.
- A novel signal amplification platform was established.
- Electrochemical recognition, catalysis, and signal amplification were realized using the same element.

GRAPHICAL ABSTRACT

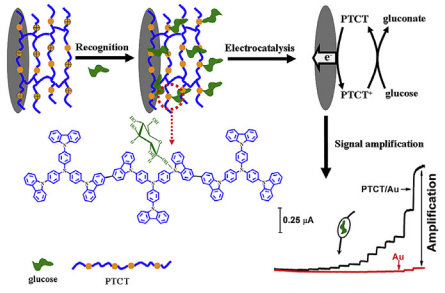

ARTICLE INFO

Article history:
Received 26 March 2015
Received in revised form
12 July 2015
Accepted 17 July 2015
Available online 8 August 2015

Keywords:
Non-enzymatic biosensor
Glucose
Signal amplification
Electrocatalysis

ABSTRACT

Hole-transporting materials with tunable structures and properties are mainly applied in organic light-emitting diodes as transport layer. But their catalytic properties as signal amplifiers in biological assays are seldom reported. In this paper, a starburst molecule, 4,4,4″-tri(N-carbazolyl)-triphenylamine (TCT), containing a triphenylamine as the central core and three carbazoles as the peripheral functional groups was designed and synthesized. Subsequently, the hole-transporting material based on the TCT polymer, poly(TCT) (PTCT), was achieved via a low-cost electrochemical method and exploited as an efficient metal-free electrocatalyst for non-enzymatic glucose detection. Here, this hole-transporting material served three purposes: electrochemical recognition (owing to hydrogen bonding interaction and the biomimetic microenvironment created by the polymer), electrocatalysis (owing to the hole-transporting capability of triphenylamine and the catalytic property of carbazole), and signal amplification (owing to energy migration along the conductive polymer backbone). The electrocatalytic and sensing performances of the sensor based on PTCT were evaluated in detail. Results revealed that the PTCT film could efficiently catalyze the oxidation of glucose at a less-positive potential (+0.20 V) in the absence of any enzymes. The response to glucose was linear in the concentration range of 1.0–6000 μM, and the

* Corresponding author.
** Corresponding author.
E-mail addresses: zzq@jlu.edu.cn (Z. Zhang), yangming1967@163.com (M. Yang).

http://dx.doi.org/10.1016/j.aca.2015.07.024

detection limit was 0.20 μM. With good stability and selectivity, the proposed sensor could be feasibly applied to detect glucose in practical samples. The encouraging sensing performances suggest that the hole-transporting material is one of the promising biomimetic catalysts for electrocatalysis and relevant fields.

1. Introduction

Glucose is a key metabolite for living organisms, especially in the case of patients suffering diabetes. Its electrochemical determination is extremely important in many areas such as clinical diagnostics, biotechnology, and the food industry [1]. Since Clark and Lyons reported the first biosensor for continuous monitoring of glucose in 1962 [2], various biosensors comprising glucose oxidase have been extensively developed [3,4]. Although enzymatic biosensors usually show good selectivity and high sensitivity, their poor stabilities originated from the intrinsic nature of enzymes remain as problems for real sensor applications. Consequently, increasing interest has been focused on the direct electrocatalytic oxidation of glucose at an enzyme-free electrode [5,6]. Early researches aimed at the use of different kinds of metal materials, including bismuth film [7], nickel complexes [8], gold [9], platinum [10,11], and copper [12,13]. However, there are several drawbacks associated with these metal-based methods. For example, the dissolution of metal ions and the toxicities of heavy metal elements involved prevent these sensors from being put to practical use. And additionally, the most common problem for metal-based sensors is the poor reproducibility due to the accumulation of adsorbed intermediates. Another disadvantage is that they lack the essential selectivity for glucose. Some structurally similar organic substances are also simultaneously oxidized along with glucose at the surface of metal materials and generate interfering signals.

The non-metallic materials with low production costs can be explored as the candidates in the hope of developing effective enzyme-free sensors. Nevertheless, at present the non-metallic glucose sensors are always based on potentiometric and capacitive principles [14] because the conductivity and catalytic activity of the non-metallic materials are relatively low. Freund et al. report a strategy that exploits aniline boronic acid as sensing elements to detect glucose [15]. Though this sensor has the merits of low cost and environmental insensitivity, some shortcomings involving unsatisfactory activity and selectivity are still existed. Park's group fabricates an amperometric glucose sensor using ferrocene as probe molecule [16]. Since the response of this system is based on the decrease in ferrocene current, its sensitivity and reproducibility are not entirely satisfactory. Furthermore, electrooxidation of glucose at non-metallic materials is usually plagued by sluggish electron transfer kinetics. It needs a large overpotential to attain reasonably good sensitivity. And yet the high overpotential significantly reduces the detection selectivity, especially for biological samples. It is therefore desirable to develop novel non-metallic materials with high catalytic activities for the electrooxidation of glucose.

The sensor performance essentially depends on three characteristics of the electrocatalysts used: stability, catalytic activity, and selectivity. In the light of this, the triphenylamine-based starburst molecules, which have been employed as hole-transporting materials in organic light-emitting diodes [17,18], may be used as novel electrocatalysts for biosensor fabrication. Firstly, the triphenylamine derivatives possess good film-forming capabilities. The polymer films based on triphenylamine always exhibit excellent structural and phase stability [19]. Secondly, the strong electron-donating ability of triphenylamine gives the polymer a decreased oxidation potential and an enhanced electrocatalytic activity [20]. In addition, the key component of biosensors is a recognition element capable of recognizing a specific target molecule. In this system, the triphenylamine molecule was functionalized with carbazolyl groups to provide recognition sites for glucose. The non-planar characteristic of the triphenylamine molecules prevented interaction or close stacking among analytes, creating a biomimetic microenvironment for the electrochemical recognition process.

A central challenge in biosensor is to amplify the signals produced in recognition process. Various signal amplification strategies have been developed, such as rolling circle amplification, enzyme labeling amplification, and polymerase chain reaction. However, the practical applications of such enzyme-based methods are limited due to environmental instability and high cost. In this respect, the molecular wire theory is an attractive alternative. Swager et al. [21] firstly establish this concept and point out that the conjugated polymers are interconnecting as a molecular wire, in which the energy migration may occur along the polymer chain due to the conductivity of the backbone. Consequently, the conjugated polymer-based system produces a response larger than that afforded by the small molecular-based system. Although this theory has been used to fabricate optical devices [22], its applications in electrochemical sensors are seldom reported, possibly because of the complicated sensing mechanisms in electrochemistry. Here, the triphenylamine and carbazolyl units were coupled into one molecule to tune the energy levels and made it qualify for the energy transfer process. And then its conjugated polymer was achieved via a simple electrochemical method. The electrons could delocalize over all the conjugated branches through the central triphenylamine unit, and the electrochemical signal was thus amplified.

In this work, a small star-shaped molecule, 4,4,4″-tri(N-carbazolyl)-triphenylamine (TCT), was designed and synthesized. A triphenylamine core was designed as the skeletal structure and three carbazolyl groups were used as the dendrons. Subsequently the hole-transporting material based on TCT polymer, poly(TCT) (PTCT), was successfully obtained via a simple electrochemical method and exploited as an efficient sensing material for the detection of glucose. In this system, the PTCT film performs three major functions: (1) Non-planar growth of the conductive film provides a three-dimensional space, and then the electrochemical recognition process between glucose and anchoring points can be carried out in a biomimetic microenvironment. (2) The hole-transporting ability of triphenylamine as well as the electrocatalytic property of carbazole is used to construct a positively charged catalytic environment, which is very beneficial to glucose oxidation. (3) The multi-branched structures of the polymer can effectively amplify the electrochemical signals. Although the hole-transporting material has been used in organic luminescent devices, its potential application in electroanalysis has not been sufficiently investigated. As an example, here we proposed an application of hole-transporting material in the fabrication of an electrochemical glucose biosensor.

2. Experimental

2.1. Reagents and apparatus

Tris(4-iodophenyl)amine and carbazole were purchased from Aldrich (USA). Copper powder, dichloromethane (DCM), acetonitrile (ACN), and glucose were all purchased from Shanghai Chemical Reagent Company (Shanghai, China). All reagents were of analytical grade and used without further purification. Doubly distilled water was used in this experiment throughout.

^{1}H NMR spectra were measured on a Bruker Avance III model 300 MHz solid-state NMR spectrometer (Bruker, Switzerland) at a MAS rate of 5 kHz. FT-IR spectra were recorded on a FT-IR-8700 spectrometer (Shimadzu, Japan). UV–visible spectra were carried out on a Shimadzu UV-2550 spectrophotometer (Shimadzu, Japan). Scanning electron microscopy (SEM) images were obtained using a SSX-550 scanning electron microscope (Shimadzu, Japan). All electrochemical measurements were performed with a CHI 920C electrochemical workstation (CH Instrument, Shanghai, China). The electrochemical cell consisted of a three-electrode system with Au disc electrode (geometric surface area 0.031 cm^2) as the working electrode and a platinum wire as the counter electrode. The reference electrode used in aqueous solutions was saturated calomel electrode (SCE), whereas Ag wire electrode was used in organic solutions (Its potential is about 0.030 V versus SCE). All electrochemical experiments were performed under a nitrogen atmosphere at room temperature.

2.2. Synthesis of the TCT monomer

TCT was prepared according to the previous reports with a slight modification [19,23]. Briefly, a mixture of tris(4-iodophenyl)amine (9.340 g, 15.00 mmol), carbazole (10.03 g, 60.00 mmol), copper powder (0.7500 g, 11.80 mmol), and K_2CO_3 (16.20 g, 117.2 mmol) was suspended in 40.00 mL of nitrobenzene. The mixture was refluxed for three days. The hot solution was filtered, and the filtrate was added dropwise in methanol. The precipitate was then filtered and washed with water and methanol successively. Finally, the precipitate was redissolved in benzene and purified through a silica gel column with a gradient solvent of hexane to hexane/toluene (3:2) as eluent to afford a slightly brown solid.

2.3. Sensor fabrication

Prior to the surface modification, the bare Au electrode was carefully polished with aqueous slurries of alumina powders (1.0, 0.3, and 0.05 μm) on a polishing cloth until a mirror surface was obtained. Then, it was washed successively with 1:1 nitric acid, ethanol, and water in an ultrasonic bath and dried under a stream of nitrogen. Subsequently, the PTCT thin film was deposited on the Au electrode by cyclic sweeping from −2.0 to +1.8 V (versus Ag wire) at 0.10 V s^{-1} for five cycles. The electrolyte used was ACN/DCM (2:3, by volume) containing 100.0 mM $LiClO_4$ as supporting electrolyte and the concentration of TCT was 1.000 mg mL^{-1}. After polymerization, the electrode was washed with ACN to remove the supporting electrolyte and monomers. The glucose sensor, poly(TCT) modified Au electrode (PTCT/Au), was obtained.

3. Results and discussion

3.1. Electrochemical preparation of the PTCT film

The successive cyclic voltammograms (CVs) of TCT electrochemically deposited onto the Au electrode are shown in Fig. S1. The TCT monomer exhibits two redox processes attributed to its polaronic and bipolaronic states, respectively [24]. This phenomenon is similar to the behavior observed for carbazole [25] and N-vinylcarbazole [26]. But due to the effect of steric hindrance, TCT oxidizes at a much higher potential than these two monomers. The shoulder peak corresponding to the doping process of the growing polymer thin films locates at about 1.20 V [27]. Result indicates that even though three carbazolyl units are included in the TCT monomer, the formation of trimer is hampered by the large steric hindrance. In fact, the electropolymerization reaction of TCT involves one or two carbazolyl units according to its charge density. Therefore, two different polymerization processes occur and a proposed mechanism is presented in Fig. S2.

3.2. Characterizations of TCT monomer and PTCT film

^{1}H NMR spectrum of TCT is exhibited in Fig. 1A. ^{1}H (300 MHz, $CDCl_3$, δ): 8.17 (d, 6H, $J = 8.1$ Hz), 7.60–7.42 (m, 24H), and 7.31 (t, 6H, $J = 7.5$ Hz) [23]. As observed in Fig. 1B, the FT-IR spectra of TCT (a) and PTCT (b) display some differences. For TCT, the peak at 1228 cm^{-1} is attributed to the C–N bonds [27], and the peaks at 746 and 721 cm^{-1} are due to the out-of-plane C–H vibration of the unsubstituted carbazole [28]. But for the PTCT film, the stretching vibration peaks for C–C and C–N are observed in the range of 1600 to 1450 cm^{-1}. The vibration peak at 1035 cm^{-1} is an indicator of the doping of the film with perchlorate anions, entering the polymer from the supporting electrolyte [25]. The peaks at 746 and 721 cm^{-1} do not appear in the FT-IR spectrum of PTCT, indicating the polymerization happened [27]. The peaks observed at 794 and 733 cm^{-1} are due to the 1,2,4-trisubstitution of benzene ring [28]. These observations suggest that polymer films are formed during the electropolymerization of TCT and the polymerization proceeds from 3,6-positions of the repeated carbazolyl units (see Fig. S2). The phenomenon is in agreement with previous reports concerning the electrochemical polymerization of carbazole and its derivatives [29,30].

The UV–visible spectra of TCT monomer and its polymer films are illustrated in Fig. 1C. The TCT monomer exhibits an absorption band with a maximum at 341 nm attributed to π–π^* transition of the carbazolyl units [31]. After polymerization, the absorption band at 341 nm still exists but its intensity decreases. This phenomenon can be attributed to the reduced carbazole radical ions and the relatively higher asymmetry in the polymer film [32]. Besides, a new broad band appears around 620 nm, which is assigned to the oligomers formed during the electropolymerization.

The polymer film exhibits a nano-/microwire-like structure (Fig. 1D), which is consistent with the molecular wire theory mentioned above. The linear growth of TCT is attributed to the steric effects of the oligomer. At the surface of the microwire-like structure, a spongy stratified structure can be observed. This morphology can facilitate electron transfer and increase active area of the obtained sensor, leading to an increase in its catalytic efficiency.

3.3. Impedance analysis

The features and impedance changes of electrode surfaces during the modification process were effectively probed by electrochemical impedance spectroscopy (EIS). Fig. 2A shows the Nyquist plots at the bare Au electrode and the PTCT/Au in the presence of 10.00 mM $Fe(CN)_6^{3-/4-}$ and 100.0 mM KCl. Both the Au and the PTCT/Au show semicircle portions at higher frequencies and linear parts at lower frequencies. The charge transfer resistance (R_{ct}) at the electrode surface is equal to the semicircle diameter in the plot and can be deduced by fitting the impedance data using the equivalent circuit (inset of Fig. 2A). For the Au electrode (a), the R_{ct} value is estimated to be 359.6 Ω. But for the PTCT/Au, the R_{ct} value

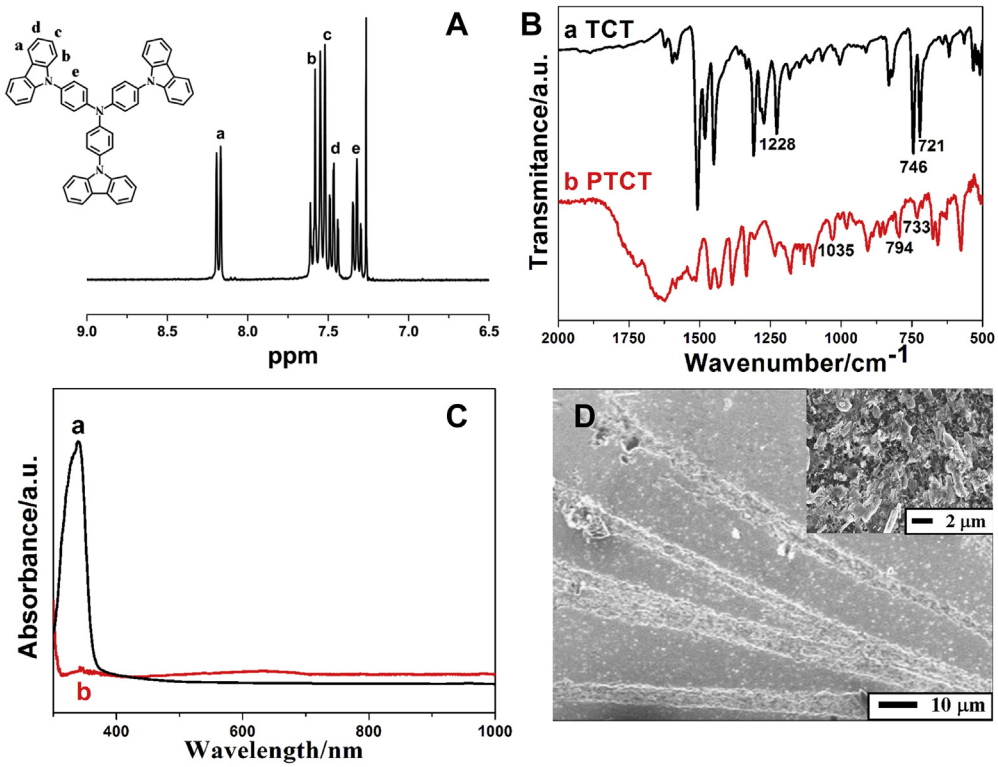

Fig. 1. (A) ^{1}H NMR spectrum of TCT monomer in $CDCl_3$. (B) FT-IR spectra of TCT (a) and PTCT (b). (C) UV–visible spectra of TCT (a) and PTCT (b). (D) SEM images of the PTCT film.

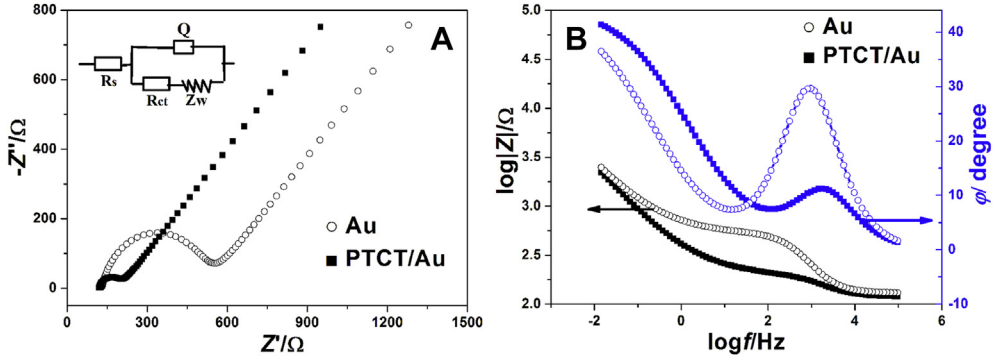

Fig. 2. (A) Nyquist diagrams and (B) Bode plots of 10.00 mM $Fe(CN)_6^{3-/4-}$ containing 100.0 mM KCl solution at the bare Au (○) and the PTCT/Au (■). Inset of (A) is the equivalent circuit. R_s: bulk resistance, R_{ct}: charge transfer resistance, Q: constant phase element, Z_W: Warburg.

decreases dramatically to 82.9 Ω. This observation further confirms that the charge transfer rate increases upon employing the polymer film.

Further electrochemical analysis was performed using a Bode plot. As shown in Fig. 2B, only a single and symmetrical peak exists in the Bode-phase plot, which corresponds to the relaxation process of the electrode/solution interface. The PTCT/Au shows a lower relaxation than the Au electrode, implying that the reaction is more facile on the former [26]. Similar results are obtained in the Bode-magnitude plot and the impedance decreases when the polymer is assembled onto the Au electrode surface [14,33]. These EIS results demonstrate that a polymer film with high charge transfer ability is obtained.

3.4. Electrochemical behavior of the PTCT film

The electrochemical behavior of the PTCT film in a monomer-free electrolyte is shown in Fig. 3. The polymer film exhibits two redox processes. The peak currents are proportional to the square root of scan rates (Fig. 3B), indicating that the electrochemical process of the polymer is diffusion limited. But for R_{e1}, the plot deviates from linearity beyond scan rate of 0.50 V s^{-1}, suggesting a thin-layer behavior. Some workers ascribe this behavior to the formation of a surface layer, like a passive layer or fouling. The similarities between the corresponding CVs in the presence (Fig. S1) and absence (Fig. 3) of monomer indicate that the redox behavior in the growing polymer is similar to that of the final film [34].

The CVs of redox probe, $Fe(CN)_6^{3-}$, can provide important information for evaluating the electrochemical properties of electrode materials. As shown in Fig. S3, the PTCT/Au gives a larger current response in comparison with the bare Au electrode. This should be attributed to the large effective area of the PTCT film. Furthermore, the difference in potential between the anodic and

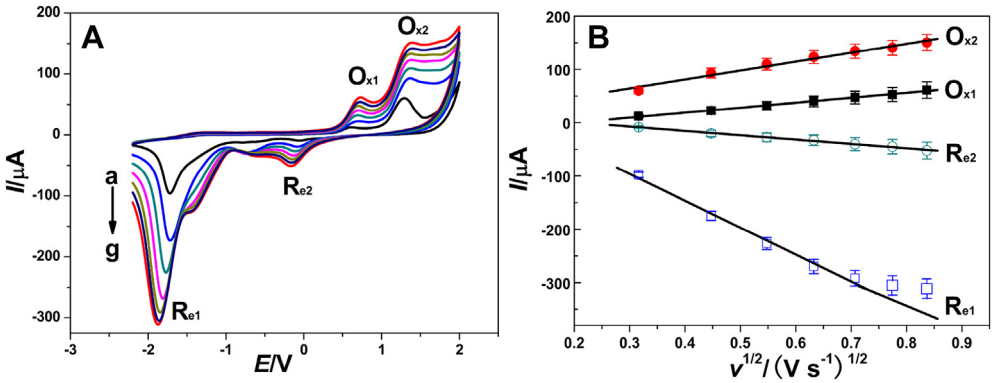

Fig. 3. (A) CVs of the PTCT/Au in a monomer-free electrolyte (ACN/DCM, 2:3) at different scan rates. (a–g): 0.10, 0.20, 0.30, 0.40, 0.50, 0.60, and 0.70 V s^{-1}. (B) Plots of peak current versus $v^{1/2}$.

cathodic peaks for ferricyanide at the PTCT/Au is 75 mV, which is 7 mV smaller than that observed at the Au electrode. The improved reversibility further illustrates that the charge transfer property of the sensor is increased.

3.5. Electrocatalytic amplification strategy for glucose sensing

3.5.1. Electrochemical behavior of glucose at the PTCT/Au

The cyclic voltammetric responses of the PTCT/Au and the Au in the presence (a and b) and absence (c) of glucose in 100.0 mM NaOH are shown in Fig. 4A. The two electrodes exhibit similar electrochemical response to glucose (a and b). But the PTCT/Au offers a higher peak current (I_{pa}) and a lower oxidation potential (E_{pa}), indicating that the PTCT film can serve simultaneously as a current amplifier and an electrocatalyst. In alkaline solvent, the glucose molecule was first electrochemically adsorbed on the surface of PTCT by dehydrogenation (Peak I). The dehydrogenated molecule could be transformed to gluconate either by direct oxidation or through a δ-gluconolactone intermediate step (Peak II). The δ-gluconolactone desorbed slowly and eventually became gluconate as a result of hydrolysis in the basic media [6]. Nevertheless, the intermediate process was not easily distinguishable at room temperature. Only at a low scan rate (e.g. 5 mV s^{-1}), two separate oxidation peaks could be observed. At higher potentials, glucose oxidative adsorption was inhibited. Then during the cathodic scan, with lower potential glucose could be adsorbed and oxidized again, generating the oxidative peak on the reverse scan (Peak III) [35]. Moreover, the electrocatalysis of PTCT toward glucose with different concentrations is also investigated. As shown in Fig. 4B, the oxidation current gradually increases with the increasing concentration of glucose, implying a possibility of quantitative determining glucose using the PTCT/Au.

In this sensing system, the PTCT film performs three major functions: electrochemical recognition, electrocatalysis, and signal amplification (Scheme 1). Firstly, the glucose is absorbed on the surface of the PTCT film through hydrogen bonding interaction. This is the electrochemical recognition process. The hydrogen atoms of glucose interact with the nitrogen atoms of PTCT chain, which is more stable than that with gold atom. The hydrogen bonds presented near the sensor surface can stimulate a faster dehydrogenation rate in the glucose oxidation, which speeds up the kinetics of the whole reaction. As a result, the intermolecular charge transfer between glucose and PTCT can be realized more effectively. Secondly, the strong electron-donating abilities of triphenylamine and the catalytic properties of carbazole give the TCT molecular a relatively low ionization potential. Consequently, the TCT-based polymer can be positively charged at a less-positive potential, which is very beneficial to glucose adsorption as well as the following oxidation processes. As observed in Fig. 4, the oxidation potentials of glucose at the PTCT/Au are negatively shifted compared with the bare Au electrode ($\triangle E_{p1}$ = 98 mV, $\triangle E_{p2}$ = 42 mV, $\triangle E_{p3}$ = 12 mV), which proves the electrocatalytic effect of PTCT for glucose oxidation. Thirdly, the conjugated and highly delocalized π-bonds in the polymer film greatly increase the mobility of electron. As a result, an efficient energy migration may occur along the conductive polymer backbone and an amplified electrochemical signal is thus obtained. Besides, a relatively high amplification factors achieving in our system can also be attributed

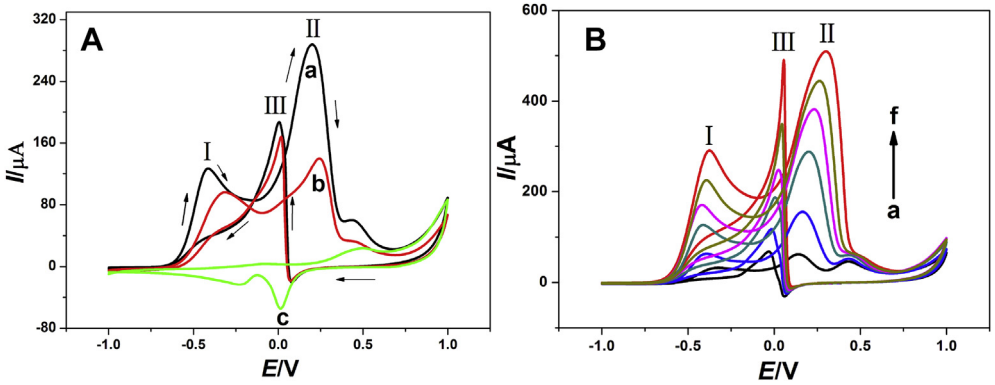

Fig. 4. (A) CVs of the PTCT/Au (a and c) and the Au (b) in 100.0 mM NaOH in the presence (a and b) and absence (c) of 15.00 mM glucose, respectively. Scan rate: 0.10 V s^{-1} (B) CVs of the PTCT/Au in 100.0 mM NaOH in the presence of glucose with different concentrations. (a–f): 5.000, 10.00, 15.00, 20.00, 30.00, and 40.00 mM. Scan rate: 0.10 V s^{-1}.

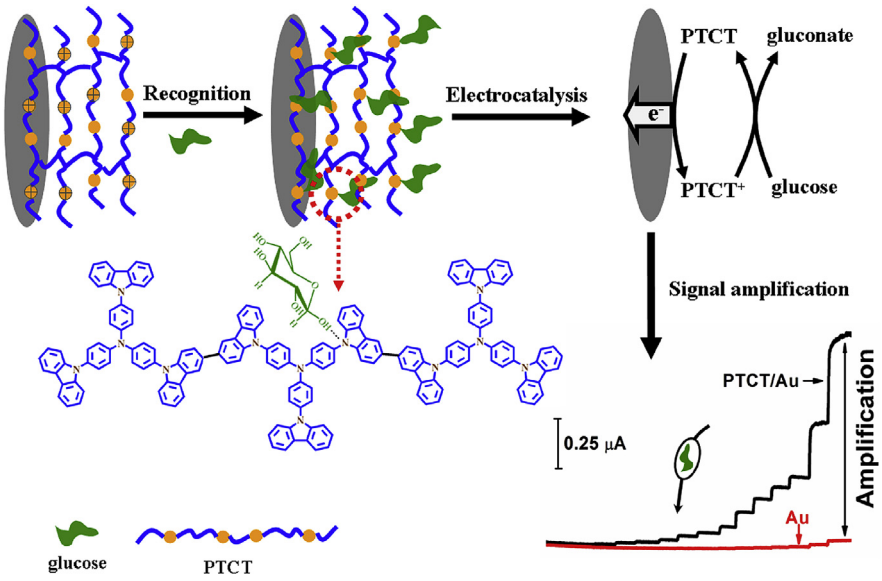

Scheme 1. Illustration of the catalytic amplification strategy for the detection of glucose.

to the large active area of the polymer film. Because the greater number of possible energy migration pathways, the higher migration rate is obtained. The detailed mechanisms of glucose oxidation at the PTCT/Au are presented in Supplementary Material.

3.5.2. Effect of the potential limit

In order to elucidate the function of the PTCT film in this catalytic reaction, the effect of the potential limit on the oxidation currents of glucose was investigated. As shown in Fig. S7A, when the lower potential limit is increased, the oxidation Peak I is noticeably lowered. It is because the reaction rate of Reaction 1 (see Supplementary Material) is assumed to be proportional to the surface concentration of adsorbed glucose, and the adsorption is a function of applied potential and glucose concentration [36]. Therefore the electrode surface becomes less adsorptive as the potential applied increases [6]. In contrast, the Peaks II and III are not affected by the lower potential limit, even when the lower limit is higher than 0 V. This behavior suggests that, the adsorption process of reactants occurs simultaneously with their oxidation reaction and takes place in the same window of potential [37]. As a consequence, glucose can be detected under a constant applied potential. Fig. S7B shows the effect of the upper potential limit on Peak III. As long as the upper potential limit is increased up to 0.25 V, which is lower than the potential where the gold hydroxide is produced, the glucose oxidation peak can be clearly seen in the negative-going scan. This observation implies that gold hydroxide is not necessary toward glucose oxidation, and it is the PTCT film that plays a crucial role in this catalytic reaction.

3.5.3. Effect of scan rate

To understand the kinetic characteristic of glucose oxidation at the PTCT/Au, we investigated the dependence of peak current on scan rate (v) (Fig. 5A). With the increase of the scan rate, the Peaks I and II show similar tendency and the peak currents are proportional to the square root of the scan rate. The linear regression equation can be expressed as I_{pa1} (μA) = $220.1v^{1/2}$ (V s^{-1})$^{1/2}$ + 21.3 and I_{pa2} (μA) = $1066.2v^{1/2}$ (V s^{-1})$^{1/2}$ + 4.2, respectively. These results indicate that the reactions are diffusion controlled processes. By contrast, the behavior of the anodic Peak III is much different owing to its non-elementary reaction process (see Supplementary material for details). According to the following equation for a totally irreversible diffusion controlled process [38]:

$$I_p = \left(2.99 \times 10^5\right) n_1[(1-\alpha)n_{\alpha 1}]^{1/2} A D^{1/2} C v^{1/2} \quad (1)$$

the diffusion coefficient, D, is calculated to be 3.21 × 10^{-6} cm^2 s^{-1}. We use only the values of Peak I due to uncertainty of the concentration for the second step.

3.5.4. Catalytic kinetic analysis

We further estimated the electrocatalytic rate constant of glucose oxidation (k_{cat}) by chronoamperometry (Fig. 5B). When the oxidation current is dominated by the rate of electrocatalytic reaction, the catalytic current can be expressed by the following equation [39]:

$$I_{cat}/I_L = \pi^{1/2}(k_{cat}Ct)^{1/2} \quad (2)$$

where I_{cat} and I_L are the currents in the presence and absence of glucose at the elapsed time t, respectively. From the slope of the I_{cat}/I_L versus $t^{1/2}$ plot (inset of Fig. 5B), the mean value of k_{cat} can be evaluated as 5.38 × $l0^5$ cm^3 mol^{-1} s^{-1}. The k_{cat} value is higher than the sensor based on metal materials [40], indicating the high catalytic activity of PTCT.

3.6. Analytical performance of the PTCT/Au in glucose sensing

3.6.1. Optimal condition

The choice of the detection potential is necessary to achieve the lowest detection limit and avoid the possible interferences. The amperometric current response of glucose at the PTCT/Au was recorded at different detection potentials. As shown in Fig. S8, the oxidation current of glucose enhances gradually with increasing the potential from 0 to +0.20 V. When further increasing the applied potential, the current shows a decreasing tendency. Thus, a constant potential of +0.20 V is selected and employed for all the subsequent amperometric detections. This detection potential is more negative than that of the non-enzymatic glucose sensors based on metal materials [9,11,41,42], suggesting that the PTCT film has a preferable electrocatalytic activity for glucose oxidation.

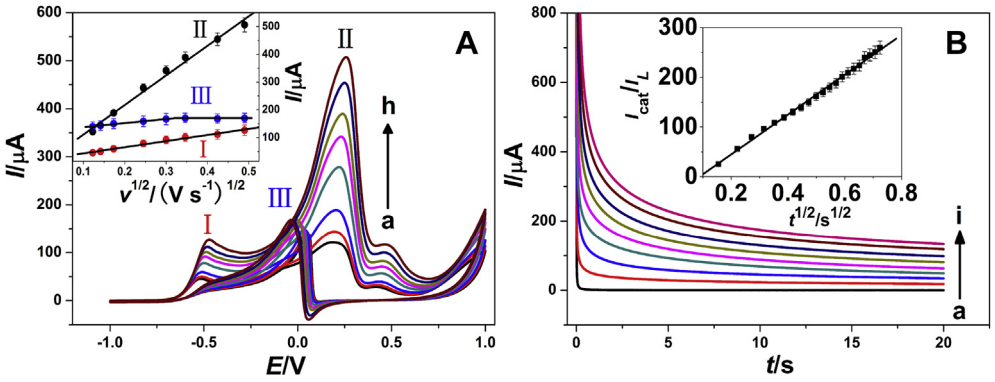

Fig. 5. (A) CVs of 20.00 mM glucose at the PTCT/Au in 100.0 mM NaOH at different scan rates. (a–h): 0.015, 0.020, 0.030, 0.060, 0.090, 0.12, 0.18, and 0.24 V s^{-1}. Inset: plots of peak current versus $v^{1/2}$. (B) Chronoamperograms recorded for the PTCT/Au in 100.0 mM NaOH with various concentrations of glucose. (a–i): 0, 5.000, 10.00, 15.00, 20.00, 30.00, 40.00, 50.00, and 60.00 mM. Inset: plot of I_{cat}/I_L versus $t^{1/2}$.

3.6.2. Amperometric analysis

Amperometric analysis was carried out at the PTCT/Au by successive injection of glucose to 100.0 mM NaOH solution. The performance of the bare Au electrode was also examined for comparison. As shown in Fig. 6A, the current at the PTCT/Au (a) increases with the increment of glucose concentration, which is much higher than that at the Au electrode (b). Calibration curves of glucose at the two electrodes are depicted in Fig. 6B. The sensitivity of the PTCT/Au is 20 times enhanced compared with that of the Au electrode, suggesting that a signal amplification platform for sensitive detection of glucose is successfully established. The linear range at the PTCT/Au is from 1.000 to 6000 μM, and the linear regression equation is I_{pa} (μA) = 0.1172 + 0.3985 C (mM) (R^2 = 0.9910) with a detection limit of 0.2000 μM (S/N = 3).

In order to make a realistic comparison with previous reports, the performance characteristics of different electrochemical methods for glucose determination are summarized in Table 1. It can be seen that the composites based on gold and copper have superior sensing properties compared to other metal materials. But most of the copper-based sensors require rather positive potentials to achieve good sensitivity (e.g., CuO nanospheres, Cu nanowires). As a result, the coexistence of interferents with glucose in the physiological system will significantly influence the practical glucose detection. Gold nanoparticle has been presented as an alternative to solve this problem, whereas it is also limited with respect to the cost and complexity (e.g., Au nanowire, three-dimension Au film). Therefore, the ability to determine glucose with high selectivity and sensitivity is still a major target. In this system, the sensor combines the hole-transporting ability of PTCT with the signal amplification effect of polymer, allowing sensitive quantification of glucose with a less-positive potential. Compared with the glucose sensors based on metal materials, the PTCT-based sensor shows higher or at least comparable sensing performance in view of detection limit and operational potential. This result demonstrates that the PTCT film is a promising non-metallic electrocatalyst for glucose oxidation, although some metal nanowires exhibit good catalytic activity.

3.7. Stability, reproducibility, and selectivity

The stability of the sensor in storage conditions (in the air at 4.0 °C) was tested by measuring the glucose solution every two days with the corresponding results shown in Fig. S9. The electrode retained 96% of its initial response current after thirty days. And after 60 days, 90% of its initial current response was still retained (Fig. S10). The excellent long-term storage stability can be attributed to the chemical stability of the PTCT film. Under similar conditions, the response currents for twelve replicate measurements at the same PTCT/Au yielded a relative standard deviation (RSD) of 2.5%. The current response decayed by 4.1% when the sensor was subjected to fifty potential cycles. These results reveal that the sensor has satisfactory storage stability and reproducibility.

To investigate the selectivity of the proposed method, we examined the effect of some potential interference compounds. The results suggest that 50-fold concentration of Na^+, Ca^{2+}, Mg^{2+}, Al^{3+}, Zn^{2+}, NO_3^-, Cl^-, SO_4^{2-}, 10-fold concentration of maltose, uric acid, folic acid, 3-fold concentration of oxalic acid, caffeine, and cysteine do not interfere with the signals of glucose, implying a good

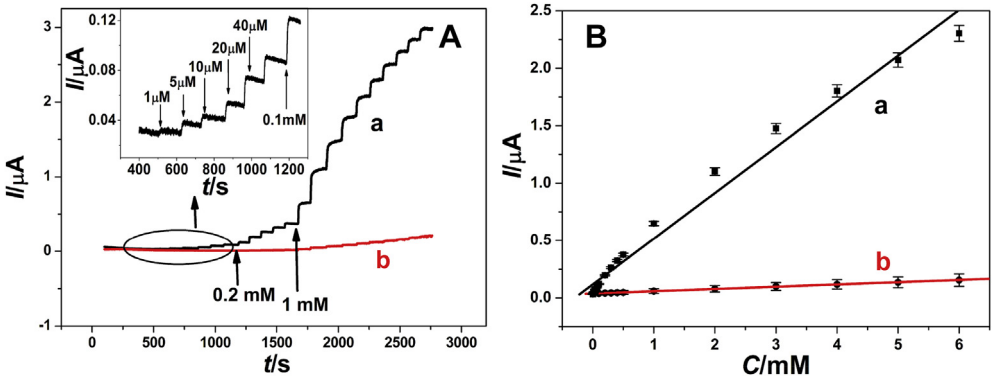

Fig. 6. (A) Amperometric response of the PTCT/Au (a) and the Au (b) on successive injection of glucose into a stirring 100.0 mM NaOH solution. The detection potential: +0.20 V. Inset A: enlarged amperometric curves. (B) Calibration curves of glucose at the PTCT/Au (a) and the Au (b).

Table 1
Comparison of several electroanalytical methods for glucose determination.

Electrode materials	Detection limit (μM)	Operational potential (V)	Linear range (mM)	Refs.
Nafion-GOD[a]-ZnO nanocomb	20	+0.80	0.02–4.5	[43]
GOD-Au-polydopamine-Fe_3O_4	6.5	−0.50	0.02–1.875	[4]
Ordered Pt nanotubes	1.0	+0.40	2.0–14.0	[11]
Pt–Pb nanowire	8.0	−0.20	1.0–11.0	[1]
NiO-graphene	5.0	+0.35	0.02–4.5	[42]
Co_3O_4-graphene	10	+0.60	0.05–0.3	[44]
CoOOH nanosheet	10.6	+0.50	0.01–0.5	[45]
FeOOH nanowire	7.8	+0.40	0.015–3.0	[46]
Porous Au	5.0	+0.35	2.0–10.0	[9]
Au nanowire	50	−0.40	1.0–10.0	[47]
Three-dimension Au film	3.2	−0.30	0.005–10.0	[48]
MPTS[b]-Au nanoparticle	0.05	+0.16	1.0–8.0	[49]
Au-NiAl-LDH[c]-CNT[d]-graphene	1.0	+0.55	0.01–6.1	[50]
Au-graphene oxide nanoribbons	5.0	+0.20	0.005–4.92; 4.92–10.0	[51]
Cu nanowires	0.035	+0.60	0.0001–2.0	[52]
Cu_xO-polypyrrole-graphene	0.03	+0.20	0.1–10.0	[53]
CuO nanowires-CNT	0.0456	+0.60	0.001–0.034; 0.034–2.67	[54]
CuO nanospheres	1.0	+0.60	0.05–2.55	[55]
PTCT	0.20	+0.20	0.001–6.0	This work

[a] Glucose oxidase.
[b] 3-mercaptopropyl-trimethoxysilane.
[c] NiAl-layered double hydroxide.
[d] Carbon nanotubes.

Table 2
Recovery of the proposed sensor in injection samples.

Sample	Added (μM)	Found[a] (μM)	Recovery (%)	RSD (%)
1	6.000	6.300	105.0	2.1
2	520.0	513.7	98.79	2.1
3	1800	1821	101.2	3.8
4	1960	1951	99.54	3.7

[a] Average of three determinations.

selectivity to glucose at the PTCT/Au. Human blood contains not only inorganic salts and proteins, but also electroactive species like ascorbic acid. Therefore, further interference tests were performed under the normal physiological level. Results (Fig. S11) show that the PTCT/Au generates insignificant response to ascorbic acid (0.1000 mM) and L-dopa (0.1000 mM) compared to the response from glucose (5.000 mM). The interference produced by hydrogen peroxide is slightly greater than other substances, which may be explained by the similar oxidation potentials of hydrogen peroxide and glucose. Consideration of the much higher concentration of glucose in blood plasma than hydrogen peroxide, the interferential response becomes negligible. By contrast, at the bare Au electrode, all these interferents generate noticeable interfering signals. These results indicate that the PTCT film can effectively improve the anti-interference ability of the sensor.

3.8. Analytical applications

In order to verify the possibility of the sensor for practical application, a freshly prepared PTCT/Au was employed to monitor glucose in various real samples, including glucose injection, human urine, blood serum, and whole blood. The blood samples are obtained from a local hospital and the urine samples are offered by healthy adult. Prior to measurements, the injection samples (standard concentration of glucose 50.00 mg mL^{-1}, 50.00 mL per injection) were diluted with water to operate in the linear range of the method. The blood serum and urine samples were diluted 200 times. And for whole blood, the original sample was diluted 1000 times to reduce the matrix effect. All the detections were carried out in separate process in 100.0 mM NaOH solution at +0.20 V. The RSD and recovery of glucose assay in injection (Table 2) and body fluids (Table 3) were assessed from three replicates. The recoveries are 96.93–105.0%. And the RSD is less than 4.0%, revealing that the proposed sensor can be employed for practical testing with favorable accuracy and precision.

4. Conclusion

In this study, a small starburst molecule, TCT, was synthesized and its polymer film was exploited as an active electrode material for direct enzyme-free glucose detection. This strategy possesses several features superior to traditional methods. Firstly, this non-enzymatic glucose sensor effectively avoids the drawbacks of enzyme electrodes, including the insufficient stability and reproducibility. The second advantage is the use of non-metallic electrocatalysts for glucose oxidation, which can minimize the interference by toxic metal ions. Finally, energy migration may occur along the conductive polymer backbone and an amplified electrochemical signal is thus obtained, revealing that the molecular wire approach can also be applied in electrochemistry. Results in this study demonstrate that the hole-transporting materials are promising electrocatalysts in sensor fabrication. Further work on

Table 3
Recovery of the proposed sensor in urine and blood samples.

Sample	Original (μM)	Added (μM)	Found[a] (μM)	Recovery (%)	RSD (%)
Urine	0	30.00	31.12	103.7	2.1
Serum	32.00	30.00	60.29	97.24	2.8
Whole blood	4.900	30.00	33.83	96.93	2.3

[a] Average of three determinations.

developing environmentally friendly materials for electrocatalysis is still desirable, and our investigation along this way is in progress. This work may provide a valuable clue to scientists who search for novel materials with potential applications in electrocatalysis and biosensing.

Acknowledgments

This work was supported by the National Natural Science Foundation of China (No. 21375045) and Natural Science Foundation of Jilin Province (No. 20130101118JC).

Appendix A. Supplementary material

Supplementary material related to this article can be found at http://dx.doi.org/10.1016/j.aca.2015.07.024.

References

[1] Y. Bai, Y. Sun, C. Sun, Pt–Pb nanowire array electrode for enzyme-free glucose detection, Biosens. Bioelectron. 24 (2008) 579–585.
[2] L.C. Clark Jr., C. Lyons, Electrode systems for continuous monitoring in cardiovascular surgery, Ann. N.Y. Acad. Sci. 102 (1962) 29–45.
[3] C. Wu, H. Sun, Y. Li, X. Liu, X. Du, X. Wang, P. Xu, Biosensor based on glucose oxidase-nanoporous gold co-catalysis for glucose detection, Biosens. Bioelectron. 66 (2015) 350–355.
[4] H. Peng, R. Liang, L. Zhang, J. Qiu, Facile preparation of novel core-shell enzyme-Au-polydopamine-Fe_3O_4 magnetic bionanoparticles for glucose sensor, Biosens. Bioelectron. 42 (2013) 293–299.
[5] S. Zhou, X. Feng, H. Shi, J. Chen, F. Zhang, W. Song, Direct growth of vertically aligned arrays of $Cu(OH)_2$ nanotubes for the electrochemical sensing of glucose, Sens. Actuators B-Chem. 117 (2013) 445–452.
[6] S. Park, H. Boo, T.D. Chung, Electrochemical non-enzymatic glucose sensors, Anal. Chim. Acta 556 (2006) 46–57.
[7] G. Wittstock, A. Strübing, R. Szargan, G. Werner, Glucose oxidation at bismuth-modified platinum electrodes, J. Electroanal. Chem. 444 (1998) 61–73.
[8] M. Yousef Elahi, H. Heli, S.Z. Bathaie, M.F. Mousavi, Electrocatalytic oxidation of glucose at a Ni-curcumin modified glassy carbon electrode, J. Solid State Electrochem 11 (2007) 273–282.
[9] Y. Li, Y. Song, C. Yang, X. Xia, Hydrogen bubble dynamic template synthesis of porous gold for nonenzymatic electrochemical detection of glucose, Electrochem. Commun. 9 (2007) 981–988.
[10] S. Park, T.D. Chung, H.C. Kim, Nonenzymatic glucose detection using mesoporous platinum, Anal. Chem. 75 (2003) 3046–3049.
[11] J. Yuan, K. Wang, X. Xia, Highly ordered platinum-nanotubule arrays for amperometric glucose sensing, Adv. Funct. Mater 15 (2005) 803–809.
[12] X. Niu, Y. Li, J. Tang, Y. Hu, H. Zhao, M. Lan, Electrochemical sensing interfaces with tunable porosity for nonenzymatic glucose detection: a Cu foam case, Biosens. Bioelectron. 51 (2014) 22–28.
[13] X. Kang, Z. Mai, X. Zou, P. Cai, J. Mo, A sensitive nonenzymatic glucose sensor in alkaline media with a copper nanocluster/multiwall carbon nano tube-modified glassy carbon electrode, Anal. Biochem. 363 (2007) 143–150.
[14] Z. Cheng, E. Wang, X. Yang, Capacitive detection of glucose using molecularly imprinted polymers, Biosens. Bioelectron. 16 (2001) 179–185.
[15] E. Shoji, M.S. Freund, Potentiometric sensors based on the inductive effect on the pKa of poly(aniline): a nonenzymatic glucose sensor, J. Am. Chem. Soc. 123 (2001) 3383–3384.
[16] S. Choi, B. Choi, S. Park, Electrochemical sensor for electrochemically inactive β-d(+)-glucose using α-cyclodextrin template molecules, Anal. Chem. 74 (2002) 1998–2002.
[17] X. Yang, H. Huang, B. Pan, M.P. Aldred, S. Zhuang, L. Wang, J. Chen, D. Ma, Modified 4,4′,4′-tri(N-carbazolyl)triphenylamine as a versatile bipolar host for highly efficient blue, orange, and white organic light-emitting diodes, J. Phys. Chem. C 116 (2012) 15041–15047.
[18] Y. Xia, J. Lin, C. Tang, K. Yin, G. Zhong, G. Ni, B. Peng, F. Gan, W. Huang, High-efficiency blue-emitting organic light-emitting devices with 4,4′,4′-tris(N-carbazolyl)-triphenylamine as the hole/exciton-blocking layer, J. Phys. D. Appl. Phys. 39 (2006) 4987–4991.
[19] Q. Liu, J. Lu, J. Ding, M. Day, Y. Tao, P. Barrios, J. Stupak, K. Chan, J. Li, Y. Chi, Monodisperse starburst oligofluorene-functionalized 4,4′,4″-tris(carbazol-9-yl)-triphenylamines: Their synthesis and deep-blue fluorescent properties for organic light-emitting diode applications, Adv. Funct. Mater 17 (2007) 1028–1036.
[20] X. Fu, C. Jia, S. Wu, X. Weng, J. Xie, L. Deng, Electrosynthesis and characterization of a novel electrochromic film based on poly(4,4′-di(N-carbazolyl) triphenylamine), Synth. Met. 188 (2014) 104–110.
[21] T.M. Swager, The molecular wire approach to sensory signal amplification, Acc. Chem. Res. 31 (1998) 201–207.
[22] G. Zhang, Y. Wen, Y. Li, J. Xu, C. Guo, B. Lu, D. Zhu, Efficient fluorescent recognition of carboxylates in aqueous media using facilely electrosynthesized poly(9-aminofluorene), J. Fluoresc. 23 (2013) 1053–1063.
[23] M.S. Liu, Y. Niu, J. Ka, H. Yip, F. Huang, J. Luo, T. Kim, A.K.-Y. Jen, Thermally cross-linkable hole-transporting materials for improving hole injection in multilayer blue-emitting phosphorescent polymer light-emitting diodes, Macromolecules 41 (2008) 9570–9580.
[24] S. Koyuncu, B. Gultekin, C. Zafer, H. Bilgili, M. Can, S. Demic, İ. Kaya, S. Icli, Electrochemical and optical properties of biphenyl bridged-dicarbazole oligomer films: electropolymerization and electrochromism, Electrochim. Acta 54 (2009) 5694–5702.
[25] M. Ates, A.S. Sarac, C.M. Turhan, N.E. Ayaz, Polycarbazole modified carbon fiber microelectrode: Surface characterization and dopamine sensor, Fiber. Polym. 10 (2009) 46–52.
[26] M. Ates, N. Uludag, Synthesis and electropolymerization of 9-(4-vinylbenzyl)-9H-carbazole on carbon fiber microelectrode: Capacitive behavior of poly(9-(4-vinylbenzyl)-9H-carbazole), Fiber. Polym. 11 (2010) 331–337.
[27] C. Xu, J. Zhao, M. Wang, C. Cui, R. Liu, Electrosynthesis and characterization of a donor–acceptor type electrochromic material from poly(4,7-dicarbazol-9-yl-2,1,3-benzothiadia-zole) and its application in electrochromic devices, Thin Solid Films 527 (2013) 232–238.
[28] H. Macit, S. Sen, M. Sacak, Electrochemical synthesis and characterization of polycarbazole, J. Appl. Polym. Sci. 96 (2005) 894–898.
[29] M. Ates, N. Uludag, A.S. Sarac, Electrochemical impedance of poly(9-tosyl-9H-carbazole-co-pyrrole) electrocoated carbon fiber, Mater. Chem. Phys. 127 (2011) 120–127.
[30] Z. Wei, Q. Wang, J. Xu, Y. Nie, Y. Du, H. Xia, Facile electrosyntheses of high tensile strength alkyl-bridged dicarbazole polymer films and its fluorescence spectra, J. Polym. Sci. Part A-Polym. Chem. 46 (2008) 5232–5241.
[31] B. Gupta, L. Joshi, R. Prakash, Novel synthesis of polycarbazole–gold nanocomposite, Macromol. Chem. Phys. 212 (2011) 1692–1699.
[32] A.S. Saraç, Ö. Yavuz, E. Sezer, Electrosynthesis and study of carbazole-acrylamide copolymer electrodes, Polymer 41 (2000) 839–847.
[33] B.J. Sanghavi, A.K. Srivastava, Simultaneous voltammetric determination of acetaminophen, aspirin and caffeine using an in situ surfactant-modified multiwalled carbon nanotube paste electrode, Electrochim. Acta 55 (2010) 8638–8648.
[34] A. Sezai Sarac, U. Evans, M. Serantoni, J. Clohessy, V.J. Cunnane, Electrochemical and morphological study of the effect of polymerization conditions on poly(terthiophene), Surf. Coat. Technol. 182 (2004) 7–13.
[35] M. Pasta, F. La Mantia, Y. Cui, A new approach to glucose sensing at gold electrodes, Electrochem. Commun. 12 (2010) 1407–1410.
[36] H. Lei, B. Wu, C. Cha, H. Kita, Electro-oxidation of glucose on platinum in alkaline solution and selective oxidation in the presence of additives, J. Electroanal. Chem. 382 (1995) 103–110.
[37] I.G. Casella, M. Gatta, M. Contursi, Oxidation of sugar acids on polycrystalline platinum and gold electrodes modified with adsorbed bismuth oxide adlayers, J. Electroanal. Chem. 561 (2004) 103–111.
[38] M. Zhou, J. Ding, L. Guo, Q. Shang, Electrochemical behavior of l-cysteine and its detection at ordered mesoporous carbon-modified glassy carbon electrode, Anal. Chem. 79 (2007) 5328–5335.
[39] J. Harrison, Z. Khan, The oxidation of hydrazine on platinum in acid solution, J. Electroanal. Chem. Interfacial Electrochem 28 (1970) 131–138.
[40] M. Guo, X. Yin, C. Zhou, Y. Xia, W. Huang, Z. Li, Ultrasensitive nonenzymatic sensing of glucose on $Ni(OH)_2$-coated nanoporous gold film with two pairs of electron mediators, Electrochim. Acta 142 (2014) 351–358.
[41] M. Li, C. Han, Y. Zhang, X. Bo, L. Guo, Facile synthesis of ultrafine Co_3O_4 nanocrystals embedded carbon matrices with specific skeletal structures as efficient non-enzymatic glucose sensors, Anal. Chim. Acta 861 (2015) 25–35.
[42] X. Zhu, Q. Jiao, C. Zhang, X. Zuo, X. Xiao, Y. Liang, J. Nan, Amperometric nonenzymatic determination of glucose based on a glassy carbon electrode modified with nickel(II) oxides and graphene, Microchim. Acta 180 (2013) 477–483.
[43] J.X. Wang, X.W. Sun, A. Wei, Y. Lei, X.P. Cai, C.M. Li, Z.L. Dong, Zinc oxide nanocomb biosensor for glucose detection, Appl. Phys. Lett. 88 (2006) 233106.
[44] X. Wang, X. Dong, Y. Wen, C. Li, Q. Xiong, P. Chen, A graphene–cobalt oxide based needle electrode for non-enzymatic glucose detection in micro-droplets, Chem. Commun. 48 (2012) 6490–6492.
[45] K.K. Lee, P.Y. Loh, C.H. Sow, W.S. Chin, CoOOH nanosheets on cobalt substrate as a non-enzymatic glucose sensor, Electrochem. Commun. 20 (2012) 128–132.
[46] C. Xia, W. Ning, A novel non-enzymatic electrochemical glucose sensor modified with FeOOH nanowire, Electrochem. Commun. 12 (2010) 1581–1584.
[47] S. Cherevko, C.-H. Chung, Gold nanowire array electrode for non-enzymatic voltammetric and amperometric glucose detection, Sens. Actuators B-Chem. 142 (2009) 216–223.
[48] Y. Bai, W. Yang, Y. Sun, C. Sun, Enzyme-free glucose sensor based on a three-dimensional gold film electrode, Sens. Actuators B-Chem. 134 (2008) 471–476.
[49] B.K. Jena, C.R. Raj, Enzyme-free amperometric sensing of glucose by using gold nanoparticles, Chem. Eur. J. 12 (2006) 2702–2708.
[50] S. Fu, G. Fan, L. Yang, F. Li, Non-enzymatic glucose sensor based on Au nanoparticles decorated ternary Ni-Al layered double hydroxide/single-walled carbon nanotubes/graphene nanocomposite, Electrochim. Acta 152 (2015) 146–154.

[51] N.S. Ismail, Q.H. Le, H. Yoshikawa, M. Saito, E. Tamiya, Development of non-enzymatic electrochemical glucose sensor based on graphene oxide nanoribbon-gold nanoparticle hybrid, Electrochim. Acta 146 (2014) 98–105.
[52] Y. Zhang, L. Su, D. Manuzzi, H.V.E. de los Monteros, W. Jia, D. Huo, C. Hou, Y. Lei, Ultrasensitive and selective non-enzymatic glucose detection using copper nanowires, Biosens. Bioelectron. 31 (2012) 426–432.
[53] P. Moozarm Nia, W.P. Meng, F. Lorestani, M.R. Mahmoudian, Y. Alias, Electrodeposition of copper oxide/polypyrrole/reduced graphene oxide as a nonenzymatic glucose biosensor, Sens. Actuators B-Chem. 209 (2015) 100–108.
[54] J. Bao, C. Hou, Y. Zhang, Q. Li, D. Huo, M. Yang, X. Luo, A non-enzymatic glucose sensor based on copper oxide nanowires-single wall carbon nanotubes, J. Electrochem. Soc. 162 (2015) B47–B51.
[55] E. Reitz, W. Jia, M. Gentile, Y. Wang, Y. Lei, CuO nanospheres based nonenzymatic glucose sensor, Electroanalysis 20 (2008) 2482–2486.